FeelPen: A Handheld Multimodal Haptic Interface for Displaying Augmented Texture Feels on Touchscreens

Bence Levente Kodak

Thesis Report

TU Delft Delft University of Technology

Haptic Interface Technology Lab
Cognitive Robotics Department
BioMechanical Design Engineering

FeelPen: A Handheld Multimodal Haptic Interface for Displaying Augmented Texture Feels on Touchscreens

Master's Thesis Report

by

Bence Levente Kodak

5152798

to obtain the degree of

Master of Science
in Mechanical Engineering

at the Delft University of Technology,
to be defended publicly on Monday June 27, 2022 at 15:00 PM.

Student number:	5152798	
Project duration:	June 1, 2021 – June 27, 2022	
Supervisor:	Dr. Y. Vardar	
Thesis committee:	Dr. ir. D. A. Abbink,	TU Delft, Chair
	Dr. Y. Vardar,	TU Delft, Supervisor
	Dr. A. Hunt,	TU Delft, External member

TU Delft Delft University of Technology

PREFACE

> Life is like going the wrong way on a moving sidewalk. Walk and you stay put. Stand still and you go backwards. To get ahead, you have to hustle.
>
> — *Farrelly Brothers*

People who know me know that I am not a man of words. Still, I would like to thank the people who helped me get ahead on my moving sidewalk. Without them, I really would not have succeeded, so there will always be a room for them in the warmest corner of my heart.

Yasemin. I still remember the first day we met in person. You said you believe in me and I can do it. You were right. Thank you for being the lighthouse in my sea of obstacles. Sometimes you even got the waves out of my way so I could sail calmly. It seems like this cruise is not over yet. At least for a while.

David. Your enthusiasm during the Human Controller course has led me to do my final project in haptics. Being the best human controller that year was a highlight. Your Hungarian snippets in the emails made me smile every time. Thank you for teaching me how to be a good diver instructor.

Peti, Balázs and Vera. Thank you for everything. From the gym sessions in the early mornings to the board games at late nights. Our laugh was limitless, our memories are countless and our friendship will be endless. You really felt like home.

My family. Mom and dad. Lolli and Zsolti. Thank you for your continuous and relentless support through my whole life. You made it possible to pursue my dreams in another country and to go home for a weekend whenever I wanted. We always had and will always have each other.

The last thanks goes to my dog, Merlin, for teaching me how to be calm and patient.

Köszönöm.

Delft, June 2022

CONTENTS

1
PAPER

FeelPen: A Handheld Multimodal Haptic Interface for Displaying Augmented Texture Feels on Touchscreens

Bence Levente Kodak and Yasemin Vardar

***Abstract*—The ever-emerging mobile market induced a blooming interest in stylus-based interactions. However, most state-of-the-art styli are passive or display only unimodal tactile feedback. Multimodal haptic devices that simultaneously stimulate our cutaneous and kinesthetic receptors to provide immersive and realistic sensations in a virtual environment during touchscreen interactions are highly desired. To this end, we developed FeelPen, a novel handheld multimodal haptic interface for touchscreens, incorporating various actuators in a smartly designed way. A voice-coil actuator, placed along the stylus tip, simulates object compliance by modifying its stroke force. Electrovibration, generated between the stylus tip and a capacitive screen, delivers roughness and stickiness cues. In addition, temperature feedback on the fingertip is provided by a miniature thermal module. We conducted characterization experiments to determine the physical characteristics and limitations of the device, followed by a psychophysical experiment, where the perceptual dimensions of the device were extracted using the semantic differential method on a set of artificial textures. Our results revealed four tactile dimensions, with the first two related to texture surface properties, and the third and fourth dimensions linked to material softness and coldness, respectively. FeelPen opens up new dimensions for future realistic texture rendering on touchscreens.**

***Index Terms*—Haptics, multimodal device, stylus, electrovibration, perceptual dimensions**

I. Introduction

THE recent advances in pen-enabled mobile devices induced a growing interest in stylus-based interactions. Styli can enable users to sign, edit, and take notes effortlessly on a virtual document, interact with graphics software programs and virtual environments, or even play games. While our interactions with tablets and computers provide realistic visual and auditory cues, the haptic feedback capabilities are still limited. In fact, commercially available styli function passively and most state-of-the-art styli in haptics research display only unimodal tactile feedback, largely in the form of vibrations or skin-stretch [1], [2]. Imagine writing on a paper with a stainless steel pen. You feel the coldness of the steel, the roughness of the paper, as well as variations of friction and deformation while dragging across the surface. It is clear that simple vibrations cannot faithfully give back the rich tactile information we would feel when interacting with our environment in a real-life scenario.

Stimuli in real life are multimodal in nature. Our perception system incorporates cutaneous and kinesthetic receptors that work in synergy to help us perceive the rich information when touching objects, including textural and thermal properties, shape and compliance [3]. Multimodal haptic devices aim to simultaneously stimulate these multiple receptors to provide immersive and realistic sensations in a virtual environment.

Several studies proposed to display multimodal tactile feedback to increase the perceived realism of rendered textures or enhance the user experience. Culbertson et al. presented a tool-mediated system that is capable of altering the friction and roughness of an object [4]. Perceived friction is changed by altering the position of a solenoid that applies braking forces to a ball, whereas roughness cues are provided by a haptuator. Another device from Culbertson et al. uses a Phantom Omni interface with a haptuator to render friction, hardness and microscopic roughness [5]. A haptic device called MH-Pen was developed to simultaneously convey vibrotactile and force information to users while interacting with a touchscreen [6]. Nakamura et al. presented a contact pad mechanism for an electrovibration display that can provide softness sensations when pushed vertically and can give lateral force feedback when moving sideways [7].

Although these studies incorporate multiple modalities in each device, none of them includes all the relevant tactile dimensions: macro and fine roughness, friction, softness and warmness [8]. However, the extensive representation of surface material properties calls for a novel haptic interface that can simultaneously convey all major tactile dimensions to the users, with a form factor and handling already familiar to them. The challenging part of creating such a pen-type device is the arrangement of all the necessary actuators and sensors in a compact way.

In this work, we present FeelPen, the first ungrounded multimodal stylus capable of displaying sensations for all relevant tactile dimensions on a touchscreen: roughness, friction, softness and warmness. Roughness and friction cues are altered via electrostatic forces generated between the stylus tip and a capacitive touchscreen. Material softness is simulated by varying the stroke force levels of a voice-coil actuator placed inside the stylus, whereas thermal feedback on the gripping fingertip is provided by a miniature thermal module. The physical characteristics and limitations of each component are evaluated by means of characterization experiments. Lastly, we ran a human study experiment to specify the perceptual dimensions of the device by making subjects rate artificial textures on a set of adjective scales.

The outline of this paper is the following. Section II

Bence Kodak and Yasemin Vardar are with the Department of Cognitive Robotics, Faculty of 3ME, Delft University of Technology.

provides concise background information on the perceptual mechanisms of the relevant tactile dimensions. Section III elaborates on the device design, while Section IV contains the characterization experiments of its different components. Section V presents the methodology of the psychophysical experiment, which aims to find the perceptual dimensions of FeelPen. The results of the study are presented in Section VI and discussed in Section VII, with limitations and ideas for future work. Lastly, the conclusions are drawn in Section VIII.

II. Background on Human Perception

A. Perceptual dimensions

Touch sense is excellent at processing the characteristics of materials, although this process is often taken for granted. In fact, common objects can be recognized very efficiently only through haptic exploration [9]. There is a variety of perceptual properties we feel when exploring textures, often called as perceptual dimensions, which have long been investigated by researchers [8], [10], [11].

A general approach to specify perceptual dimensions is to conduct psychological experiments by collecting subjective data, then to analyze this data by multivariate analysis (factor or principal component analysis or multidimensional scaling) to extract the possible tactile factors and dimensions [8]. In general, three methods are used. In the semantic differential (SD) method, participants rate each material by using scales of individual adjectives or opposing pairs of adjectives [12]. In the similarity estimation method, participants rate the similarity of paired materials [10]. Lastly, in the classification method, participants classify the materials into different groups based on their similarities [13].

Based on the various publications reviewed, Okamoto et al. proposed five possible major psychophysical dimensions of tactile perception [8]. These are macro and fine roughness, friction, softness and warmness. Importantly, no single study reported all these five dimensions, given that the results depended on the psychological experiments, the materials used, and the analysis of the data.

One might also ask if there are any specific movements to gather information related to these dimensions. Lederman and Klatzky investigated this question and found that there exist optimal or even necessary exploratory procedures that are generally used to obtain the information about a certain material property [9]. These exploratory procedures are lateral motion for roughness perception, pressure for hardness perception and static contact for perceiving temperature.

B. Roughness and friction perception

David Katz proposed that two distinct mechanisms contribute to the tactile perception of roughness [14]. This duplex theory has been supported by the future findings of Hollins et al., where they showed that spatial cues are dominant across macro-textures (inter-element spacing $\geq 200\ \mu m$), and vibrotactile cues have a primary role among fine surfaces [15]. Other studies confirmed that, on the macro-textural level, surface roughness sensations are mainly affected by the gaps between elements, whereas the width of the elements play a less important role [16], [17]. However, temporal parameters, such as the grating temporal frequency, which depends on the scanning speed, or the root-mean-square of tangential force rate during scanning were also found to be important for roughness perception of macro-textures [18], [19]. Vibration cues are essential for fine textures, as no difference was perceived in roughness for finer textures in the absence of vibratory cues [20]. Roughness can also be well discriminated when exploring the surface with a rigid tool [21]. In this case, vibrotactile cues are dominant, and the probe tip diameter plays a role in the roughness perception of gratings.

With the growing number of haptic devices and the new possibilities of haptic texture rendering, it is important to understand whether the perception of virtual textures is similar to the real ones. Unger et al. found that the psychophysical curves for dithered conical textures rendered on a haptic device were nearly identical to those of real textures with similar geometry [22]. In contrary, Isleyen et al. showed that perceived roughness of real gratings and virtual gratings rendered on a flat electrovibration display are different, as the virtual gratings followed a decreasing trend in roughness perception with increasing spatial period [23], [24].

Next to roughness, perceived slipperiness is also a major dimension in texture surfaces, which correlates well with the kinetic friction [25]. However, the friction coefficient decreases with increasing normal load until a plateau, so the friction coefficient dominates while moderate force is applied during exploration [26].

C. Thermal perception

The sensing range of our thermoreceptors are between 5°C and 45°C, and sensation of pain occurs when the temperature falls below 15-18°C or rises above 45°C [27]. As the resting temperature of the skin is usually higher than the ambient temperature of different materials, the perceived coldness of the materials being touched is related to the rate of heat extraction from the fingers. The rate of temperature change is also an important factor, as the rapid temperature change seems to invoke the strongest coldness sensations when touching a material [28]. Furthermore, the good spatial summation of the thermal perceptual system results in a lower detection threshold for a temperature change over larger areas [29].

D. Softness perception

Moving on to softness perception, there are some differences in the perceptual mechanisms of softness with the bare finger or by using a rigid tool, for example a stylus. Tiest and Kappers showed that a large fraction of information originates from cutaneous cues when we determine the softness of materials with the finger pad [30]. This statement can be supported by the findings of Srinivasan and LaMotte, where cutaneous information alone was sufficient to discriminate the softness of objects with deformable surfaces, whereas for spring-loaded cells with rigid surfaces, both cutaneous and kinesthetic information were necessary [31]. When using a tool for softness perception, the primary cues are kinesthetic due to the absence of direct skin contact with the material [32].

Softness discrimination is better for tapping than for pressing with a stylus, as the major factor in determining compliance is the rate of change of the force applied to the skin by the stylus [33]. However, softness can also be discriminated when there is already a contact with the material, where the major factor is the ratio of the indentation depth of the stylus and the exerted force on the skin. This latter case is important for an application where we want to provide softness sensations with a tool on a rigid surface, for example, on an electrovibration display.

E. Perceptual space of artificial textures

With the development of surface haptic displays, the synthesis of a wider variety of artificial textures has become available. However, it is by no means certain that natural and artificial textures share the same perceptual dimensions. Studies conducted on both ultrasonic and electrostatic displays revealed that rough/smooth dimension is also present among artificial textures [34], [35]. Frequency is one of the key parameters in the distinction of such textures [36], [37]. Beyond frequency, waveform and amplitude are also important parameters. Dariosecq et al. proposed a two-dimensional space of textures, where roughness was influenced by waveform and amplitude, and spatial period explained the inner cluster variation within this dimension [34]. Bernard et al. composed their texture set by varying the fundamental and overtone spatial frequencies and the waveform amplitudes, and found a 2D texture space [38]. The texture set of Mun et al. using tessellations of polygons on an electrovibration display was three-dimensional, these being rough/smooth, dense/sparse and bumpy/even [35]. The question remains whether the perceptual space of artificial textures can be extended by adding thermal variation and deformability to friction modulation displays.

III. Device Design

The primary consideration in the design phase was that FeelPen should be able to deliver the sensations of various textural properties - roughness and frictional cues, temperature cues and softness - using only commercially available sensors and actuators. Moreover, when selecting the components, the balance between size and performance is a decisive aspect, as every component has to be as small as possible to fit inside a relatively compact pen. With these in mind, here we introduce the three main components and working principles of the device. Figure 1 a) shows the overall design of the device, while Figure 1 c) depicts the signal workflow between the hardware components.

A. Roughness and friction rendering

Electrovibration is a feasible solution for delivering roughness and friction cues, as studies that focused on rendering realistic textural data showed promising results in texture realism [39], [40]. Electrovibration produces wide-bandwidth forces, have fast dynamics and require low power [41]. Furthermore, Wang et al. have demonstrated the competency of using pen-type devices with an electrovibration display [42].

Here, the perceived roughness and friction cues are altered via electrostatic forces generated between the conductive stylus tip and a capacitive touchscreen (SCT3250, 3M Inc.) The alternating input voltage signal supplied to the touchscreen is first generated by a data acquisition card (PCIe-6323, NI) and then amplified via an amplifier. The stylus tip is grounded to enhance the magnitude of the electrostatic forces [43]. The DC and AC components of the voltage signal modify the constant and alternating adhesion between the stylus tip and touchscreen, respectively [44]. Hence, by changing the amplitude and frequency components of the input voltage signal, various roughness and friction sensations can be conveyed.

B. Softness rendering

The object compliance is simulated with a voice-coil actuator (VCA) with different stroke force levels. Its relatively small diameter (16 mm) makes it fit inside the housing, so we can avoid the bulky structure of some previous pen-type device designs that incorporated DC motors and rack gears for force rendering [45], [46]. A force sensor (060-2443-06, Honeywell International Inc.) measures the transmitted user's force on the stylus tip. The voltage data read by the sensor is amplified first by a load cell amplifier (HX711, SparkFun Electronics) and then sent to a microcontroller (Mega 2560 Rev 3, Arduino Inc.). The force sensor is attached to a rod that connects to the moving magnet of a voice-coil actuator (MI-MMB 1555, Magnetic Innovations Inc.) with a threaded shank. The entire mechanism moves together inside the stylus; the base of this movement is the outer shell of the voice-coil placed stably inside the housing. The stroke force of the voice-coil actuator is modified proportionally to the compliance of the emulated material. So when we push down the pen, we can feel various force levels as a function of indentation, counteracting the force generated by the actuator. The voltage input signal sent to the voice-coil actuator is amplified first by a motor driver (Motor Shield v2.3, Adafruit Inc.) to supply the necessary power.

C. Thermal rendering

Thermal cues are provided by a Peltier cell (CP076581-238, CUI Devices) placed at the finger grip location on the housing, which is driven by a compact H-bridge motor driver board (DRV8835, Pololu Corporation). As thermoelectric modules need proper cooling for thermal stability and performance, an additional heat sink need to be placed on the pen. However, natural convection heat sinks are too large to be applied inside the pen. To solve this issue, a miniature, water-cooled aluminum heat sink (overall dimensions 22x12x4 mm) was designed to dissipate the heat pumped by the Peltier cell, similar to [47]. The technical drawings of the heat sink can be seen in Appendix A. A compact water pump (480-188, RS PRO) circulates the water inside the heat sink. The heat sink and the water pump are connected with flexible silicone tubes (1030S0003414, Technirub International BV). Finally, a miniature thermistor (GA10K3MCD1, TE Connectivity) is placed on top of the Peltier cell to close the control loop of the thermal module, controlled by the Arduino microcontroller.

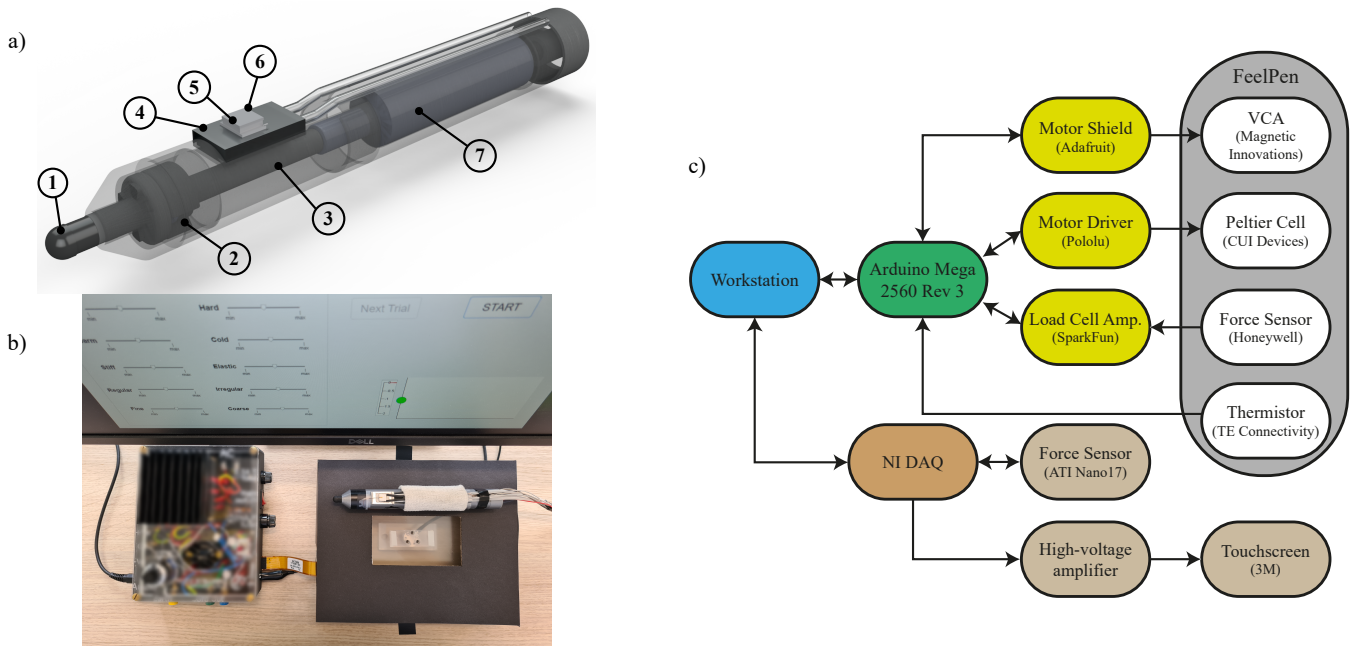

Fig. 1. Device design and apparatus of the psychophysical experiment. **a)** Electromechanical design of FeelPen: (1) capacitive pen tip, (2) force sensor, (3) connection rod, (4) water-cooled heat sink, (5) thermistor, (6) Peltier cell, (7) voice-coil actuator. **b)** Apparatus of the psychophysical experiment with the prototype of FeelPen. The touchscreen, placed on top of a force sensor, is covered by a cardboard cover with a 9x5 cm rectangular cutout on top. The LCD screen shows part of the graphical user interface. **c)** Signal workflow between the electronic components of the setup.

IV. Electromechanical Characterization

To determine the physical characteristics and limitations of the three main components of the device, we conducted characterization experiments. Based on these experiments, we can later determine which parameters to use for the rendering of distinct stimuli.

A. Thermal module performance

The goal with the thermal module is to obtain fast and accurate temperature feedback at the contact surface of the finger pad and the Peltier cell in the temperature range of 15-40 °C. The resting skin temperature is of great importance, as the differences in skin temperature can cause us to perceive the thermal cues on a display differently. Our device makes possible to set a common baseline temperature for users, thus reducing variability within and between subjects.

To control the thermal module, a PID algorithm with feed-forward control is implemented. Preliminary tests on the thermal module revealed an asymmetric system behaviour, which led to the implementation of two sets of PID controller parameters, one for heating up the finger pad and one for cooling it down (see Appendix B). The temperature control algorithm is computed on the microcontroller with a sampling frequency of 100 Hz.

The characterization of the thermal module included two experimental sessions, each session was performed in a laboratory with an ambient room temperature of 20 °C.

1) Step Response of the Thermal Module: The first experiment evaluated the temperature tracking performance and stability of the thermal module while the finger was in constant contact with the device. The initial contact temperature was set to 28 °C and step signals with four different reference temperatures (15°C, 22°C, 34°C and 40°C) were chosen to study both the cooling and heating performance of the module. Five measurements were conducted for each of the reference temperatures and metrics - settling time, overshoot and steady-state error - were calculated for each of the temperature profiles.

The step response curves and the mean step response parameter values of the first experiment are shown in Figure 2. The system was stable for all the reference temperatures. Settling time values were calculated with a 5% errorband and negative steps produced a faster tracking performance on average. The magnitudes of overshoot and steady-state error were also lower for the cooling phases.

2) Finger Contact Response of the Thermal Module: The second experiment evaluated the temperature response of the module to finger contact. With this, we calculated the time needed to reach a reference temperature once someone touches the module, as we do not want to provide further cooling or warming stimuli until the contact temperature is settled at the reference. Here, the experimenter touched the Peltier cell while a set of constant reference temperatures (15°C, 22°C, 28°C, 34°C and 40°C) were tracked. Contact time between the finger and the thermal module was at approximately 4 seconds. Five measurements were conducted for each of the reference temperatures and mean settling times were calculated.

The finger contact response curves of the second experiment are shown at Figure 3. For the cooling phase, the highest mean settling time was 2.55 s for the reference temperature of 15 °C, whereas for the heating phase, the highest mean settling time was 3.93 s for the reference temperature of 34 °C.

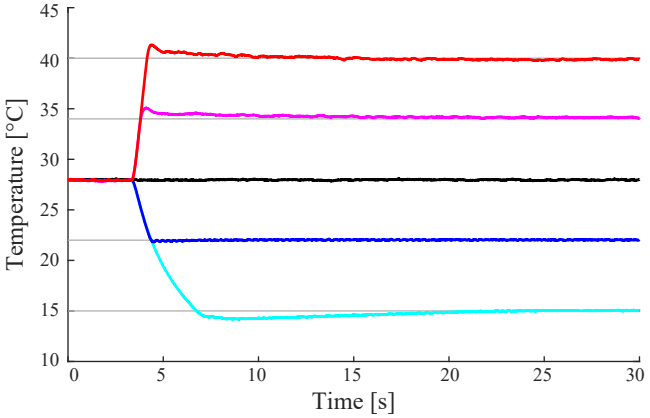

Reference temperature [°C]	15	22	34	40
Settling time [s]	9.25	0.91	14.8	2.78
Overshoot [%]	7.12	3.87	18.13	11.07
Steady-state error [°C]	0.038	0.066	0.12	0.15

Fig. 2. Step response curves and step response parameters of the closed-loop system for four reference temperatures. The gray lines represent the reference temperatures.

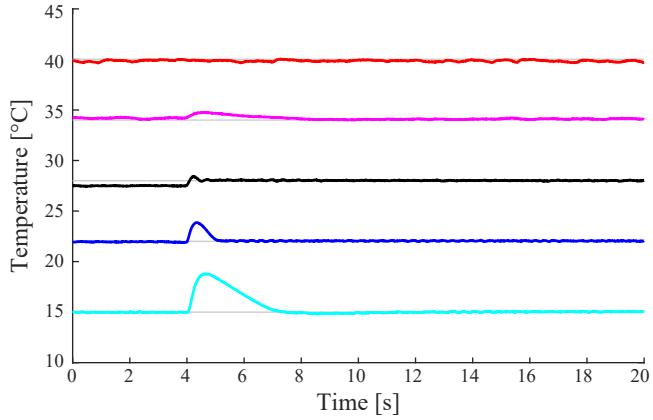

Fig. 3. Finger contact response on the thermal module, with contact at 4 seconds.

B. Force characteristics of the voice-coil actuator

Modelling and validating the force characteristics of the voice-coil actuator are essential steps for future softness rendering of the device. Here, we present the electrodynamic model of the voice-coil actuator and validate it with measurements. Moreover, we provide the maximum stroke force of the actuator as a function of indentation depth.

The force generated by the voice-coil actuator is acting based on the Lorentz principle,

$$F_{\mathrm{VCA}} = K_{\mathrm{F}}(x) \cdot I, \tag{1}$$

where $K_{\mathrm{F}}(x)$ is the force sensitivity (or force constant) of the actuator and I is the current flowing through the coil. $K_{\mathrm{F}}(x)$ is dependent on the position of the moving magnet along the cylinder axis.

Using a voltage-drive circuit, the actuator current I is indirectly controlled based on the electromechanical dynamics of the actuator:

$$E = RI + K_{\mathrm{B}}\frac{dx}{dt} + L\frac{dI}{dt}, \tag{2}$$

where E is the voltage sent to the actuator, R is the wire resistance, L is the coil inductance, $K_{\mathrm{B}} \cdot dx/dt$ is the back-electromotive force (BEMF) induced by the moving magnet inside the coil and K_{B} is the BEMF constant.

The dynamic model of the voice-coil actuator can be driven by applying Newton's second law ($F = ma$) to the moving magnet of the actuator, using Equations (1) and (2). When the mass of the moving cylinder is m and the external load on the cylinder is F_{ext}, the dynamic model is the following:

$$F_{\mathrm{VCA}} - F_{\mathrm{ext}} = m\frac{d^2x}{dt^2}. \tag{3}$$

This, using Equation 1, can also be written as:

$$K_{\mathrm{F}}(x) \cdot I - F_{\mathrm{ext}} = m\frac{d^2x}{dt^2}. \tag{4}$$

In addition to the electrodynamic model, a thermal model can also be evaluated. Heat is generated inside the coil due to the Joule effect, leading to an increase in coil resistance and thus a decrease in the maximum exerted force. However, as the voice-coil actuator operates for relatively short time periods in our application, the thermal effects were neglected and only the simpler electrodynamic model with constant coil resistance was implemented in Simulink. The parameters of the MI-MMB 1555 voice-coil actuator can be found in Appendix C.

The model is validated by simple laboratory experiments. The test bed used for force measurements consists of a force sensor (Nano17, ATI Inc.) and an adjustable frame where the pen can be placed stably in a horizontal position. Force characteristics of the voice-coil actuator were tested with a ramp voltage signal (slope 3.9 V/s, $V_{max} = 10V$) for four different positions of the moving magnet. These were the middle position of the magnet inside the stator, and 2 mm, 5 mm and 8 mm from the middle position. The voltage signals were sent to the actuator from the microcontroller at 100 Hz and the forces were sampled by a data acquisiton card (PCIe-6323, NI) at 1 kHz. Five different measurements were taken for each position.

The simulated and measured force characteristics of the actuator are shown in Figure 4 and in Appendix C. The mean absolute error (MAE) values between simulated and measured forces are presented in Table I. The validated model allows us to simulate the force values of the VCA as a function of indentation depth of the pen for different constant voltages sent to the actuator (Figure 5). The black line marks the maximum forces available with the device.

TABLE I
MEAN ABSOLUTE ERRORS (MAE) BETWEEN SIMULATED AND MEASURED FORCE VALUES

Position	Middle	2 mm	5 mm	8 mm
MAE [N]	0.054	0.093	0.057	0.03

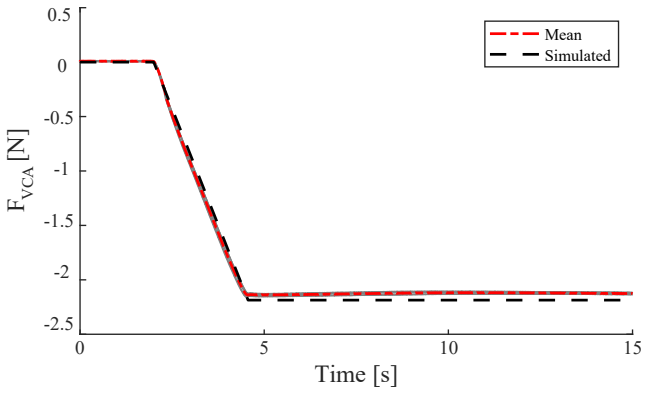

Fig. 4. Simulated and measured force characteristics of the voice-coil actuator with the moving magnet in the middle position. The grey lines represent the individual measurements.

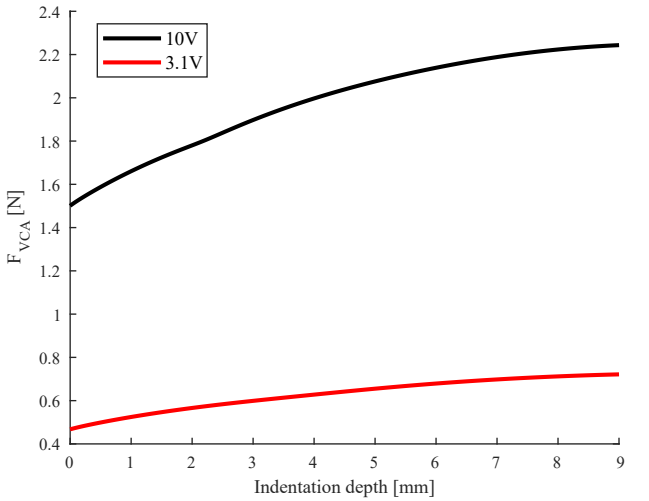

Fig. 5. VCA force - indentation depth characteristics for constant voltages. At 9 mm indentation depth of the pen, the moving magnet is in the middle position.

C. Electrostatic display - pen interaction

We characterized the pen - electrostatic display interaction to identify the electrovibration force amplitudes and the friction coefficients while scanning on the display with the device. The stimulus that induces the perception of electrovibration is the electrovibration force amplitude [48], so it is highly important to measure its dependency on voltage signal frequency and amplitude, as well as scanning speed and applied normal force. We also investigated how these parameters affect the friction coefficients.

During the sessions, one participant (the first author) sat in front of the touchscreen (SCT3250, 3M Inc.) that was attached on top of the ATI Nano17 force sensor (Figure 1 b) shows the setup). Contact forces were measured by this sensor and sampled by a DAQ (PCIe-6323, NI) at 10 kHz. The voltage signals applied to the screen were first generated with the same data acquisition card and then amplified by a custom-made high-voltage amplifier.

The input signals sent to the conductive layer of the touchscreen were zero mean sinusoidal voltage signals with various amplitudes and frequencies. Five different peak-to-peak amplitudes (40, 80, 120, 160 and 200 Vpp) and ten different frequencies, equally spaced on a logarithmic scale from 10 to 1000 Hz (10, 17, 28, 46, 77, 129, 215, 360, 600 and 1000 Hz), were tested. The participant scanned the display using two different scanning speeds (50 mm/s and 100 mm/s) and three pressing forces (0.5N, 1N, 1.5N). Contact forces for all the combinations of signal amplitude, frequency, scanning speed and pressing force were recorded (5x10x2x3 = 300 trials). In addition, six more trials were recorded without electrovibration, combining tested scanning speeds and pressing forces.

The participant scanned the touchscreen five times for each condition by holding the pen in his right hand and sliding from left to right. The sliding speed was controlled with a metronome. Each scan started at a metronome tap and ended at the next tap. After each pass, he lifted the pen from the display and returned it for the next pass. The force values were made visible with background data acquisition in a Matlab program to track the applied pressing forces. All the scanning speed and force conditions were practiced until sufficient performance before the actual experiments, ensuring that data were collected in similar manners.

To calculate kinetic friction coefficients, first lateral and normal forces were low-pass filtered with a cut-off frequency of 1 kHz. Then, the signals were segmented into five such that each one represents only the forces when sliding with approximately constant speed. After this, the lateral force segment was divided by the corresponding normal force segment and averaged to get the coefficient for each segment. The average kinetic friction coefficient for each condition was calculated by averaging the coefficients obtained from the five segments.

When applying a zero mean sinusoidal voltage signal to the touchscreen, the resulting electrovibration force occurs at twice the input signal frequency, as shown by previous studies [44], [48]. So, for example, a 10 Hz sinusoidal voltage signal on the touchscreen would produce an electrostatic force oscillating at 20 Hz. The amplitude of the electrovibration forces in both lateral an normal directions was calculated by first segmenting the force signals as in the previous case. Then, the signals were band-pass filtered with the following cut-off frequencies: $2 \cdot f_v \pm 5$ Hz for for voltage signal frequencies (f_v) from 10 to 46 Hz, and $2 \cdot f_v \pm 10$ Hz for f_v from 77 to 1000 Hz. After this, the average power of each filtered signal was calculated. Multiplying the average power by two and taking the square root of this value gave the amplitude of the electrovibration force for each segment. The average electrovibration force magnitude was calculated by averaging over the five segments for each condition.

Figure 6 shows the average kinetic friction coefficients and the average magnitude of combined (lateral and normal) electrovibration forces for different conditions.

V. Psychophysical Experiment

This experiment aimed to identify the capability of the haptic interface for rendering the major psychophysical dimensions of tactile perception. The task of each subject was

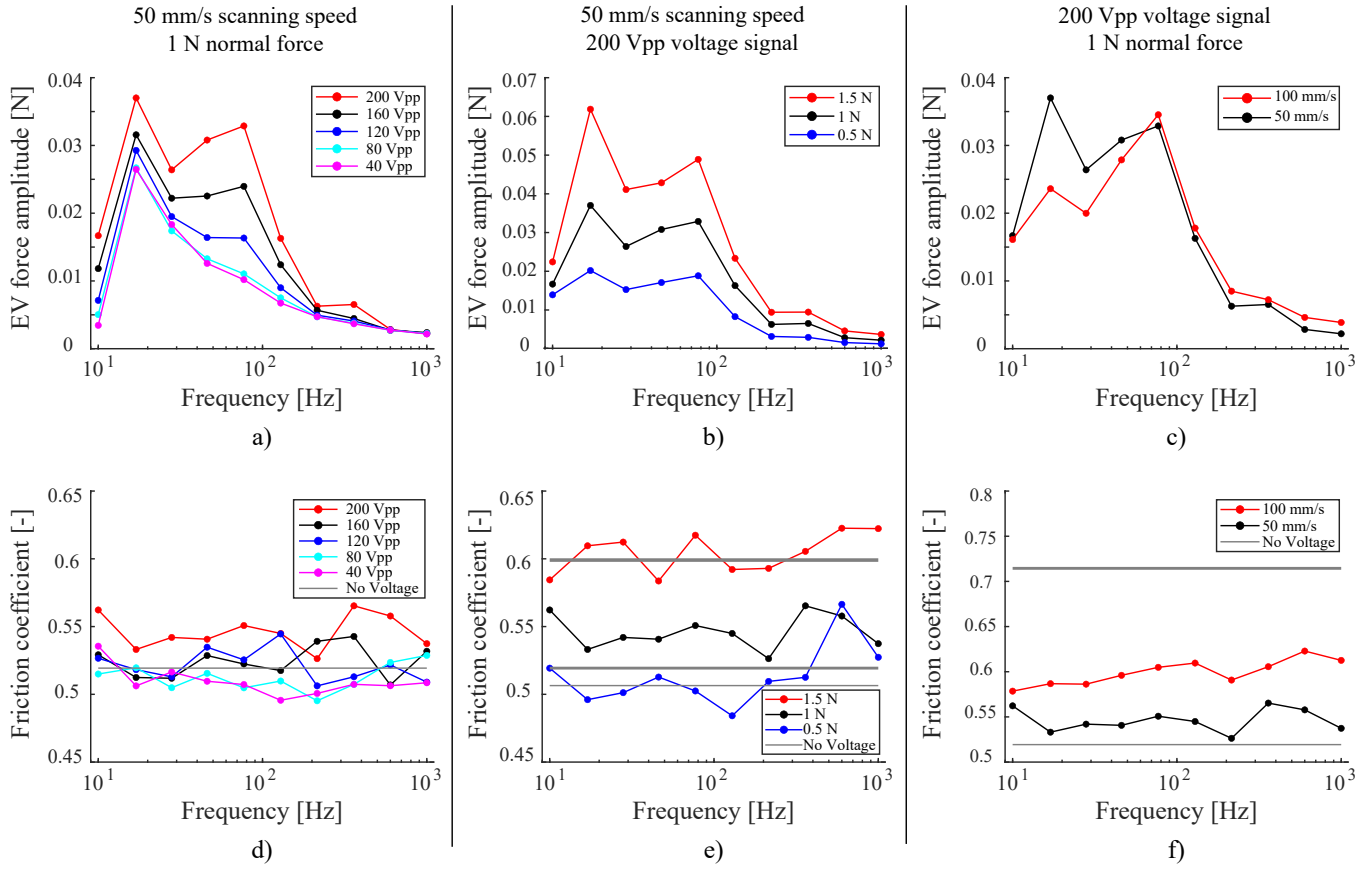

Fig. 6. Electrovibration force amplitudes and friction coefficients **a)** and **d)** as a function of voltage signal amplitude with 50 mm/s scanning speed and 1N normal force, **b)** and **e)** as a function of normal force with 200 Vpp voltage signals and 50 mm/s scanning speed, **c)** and **f)** as a function of scanning speed with 200 Vpp voltage signals and 1N normal force. The gray lines on the friction coefficient plots represent the cases where no voltage was applied to the touchscreen.

to explore various artificial textures generated with the device and rate them on a set of adjective scales. We analysed the results of the characterization experiments to provide distinct stimuli to the subjects.

A. Participants

Six women and fourteen men with an average age of 25.1 years (standard deviation, SD: 2.39) participated in the psychophysical experiment. Only two participants were left-handed and none of the participants had previous or current visual or sensory-motor disabilities. The experimental procedures were approved by the Human Research Ethics Committee (approval number 1955) at the TU Delft. All participants gave informed consent.

B. Experimental setup

Participants sat in front of a touchscreen and an LCD monitor (Figure 1). The touchscreen was attached on top of a force sensor (Nano17, ATI Inc.) that measured the contact forces. These forces were sampled by a data acquisiton card (PCIe-6323, NI) at 10 kHz. The touchscreen was covered by a cardboard case, with a 9x5 cm rectangular cutout on top. The voltage signals applied to the screen were first generated with the same data acquisition card and then amplified by a custom-made high-voltage piezo amplifier. Force and thermal feedback were controlled by a microcontroller (Mega 2560 Rev 3, Arduino Inc.) at 100 Hz. Elastic adhesive bandage was put on the middle part of the pen to avoid additional thermal stimuli on the thenar webspace from the possible heating of the voice-coil actuator. Participants also wore noise cancellation headphones (QC35 II, Bose) with pink noise to mask any auditory cues. The LCD monitor was used for interacting with a graphical user interface. Participants gave their responses with a computer mouse.

C. Stimuli

The perceptual evaluation was addressed by creating a virtual texture design space with distinguishable features that can be both mathematically and perceptually scaled. One of the advantages of using artificial textures is that we can choose and adjust their physical parameters. However, it is not so clear which are the best parameters for synthesizing distinguishable texture properties. Friesen et al. chose amplitude, frequency and irregularity of sinusoidal voltage signals as the perceptually relevant features on an electrovibration display, where irregularity refers to the width of the spectral content around the center frequency [37]. We inspired from this approach and expanded it with temperature and the stroke force of the

voice-coil actuator in order to enhance the multi-modality of the device and possibly capture the entire perceptual space of the four major tactile dimensions. To sum up, our texture design workspace was combined from five different parameters: amplitude, frequency and irregularity of sinusoidal voltage signals, temperature and stroke force of the VCA.

Parameters were selected to cover a wide spectrum of haptic stimuli. We analysed the electrovibration force magnitude plots (Figure 6) and chose amplitude (120 Vpp and 200 Vpp) and center frequency (17 Hz, 77 Hz and 360 Hz) values that induced distinct magnitudes and thus easily perceived differences.

The voltage signals were constructed from white noise that was made uniform in the [-1,+1] range. This white noise was filtered with the following filter:

$$H(z) = \frac{\frac{\sin w_0}{2Q} - \frac{\sin w_0}{2Q} z^{-2}}{\left(1 + \frac{\sin w_0}{2Q}\right) - (2\cos w_0) z^{-1} + \left(1 - \frac{\sin w_0}{2Q}\right) z^{-2}}, \quad (5)$$

where the Q-factor and w_0 are calculated as

$$Q = \frac{1}{R} \quad (6)$$

$$w_0 = \frac{2\pi f_0}{f_s}. \quad (7)$$

In Equations (6) and (7), R is the irregularity value, f_0 is the center frequency of the sinusoidal signal and f_s is the sampling frequency (10 kHz). The lower the value of the irregularity, the more the signal resembles to a simple sine wave. After filtering, the signals were divided by their upper envelopes to get a maximum amplitude of one in the time domain. The amplitude of the signal was changed by scaling. R values of 0.0001, 0.34 and 1.67 were used in the experiment, giving distinct sensations of stimuli.

When delivering thermal cues to the hand, the resting skin temperature is of great importance, as the difference of skin temperature between individuals can cause each person to perceive the thermal cues on a display differently. The constant contact between the thermal module and the index finger of the participants enabled us to set the resting skin temperature to 28 °C for each individual before each trial. From this level, at the beginning of each trial, the index finger was either cooled down to 24 °C, warmed up to 40 °C or remained at the same temperature level. Step signals were used as reference temperatures, similar as in the characterization experiments (Figure 2).

For softness sensation, two different constant voltage levels were sent to the voice-coil actuator, these being 3.1V and 10V (Figure 5). Initially, the tip of the pen was at its maximum stroke length in both cases. When the tip is indented, the one with higher voltage and thus higher generated actuator force exerts a higher force on the skin for the same indentation. This principle makes it possible to provide different softness sensations, as the major factor for softness discrimination with a tool is the ratio of the indentation depth of the tool and the exerted force on the skin.

The parameter values of the design workspace can be found in Table II. The combination of all the parameters (3x2x3x3x2) yields 108 different textures. However, to reduce the duration of the experiment, we kept only the ones that were perceptually distinct from the others. This resulted in 60 textures in total.

TABLE II
PARAMETER VALUES OF THE DESIGN WORKSPACE

Center frequency [Hz]	17, 77, 360
Amplitude [Vpp]	120, 200
Irregularity [-]	0.0001, 0.34, 1.67
Temperature levels [°C]	24, 28, 40
Voltage on VCA [V]	3.1, 10

D. Adjectives

A set of sensory adjectives was composed from the touch lexicon proposed in [49] and the adjective list in [50]. Based on preliminary tests, only sixteen sensory adjectives were chosen (see Table III).

TABLE III
SET OF ADJECTIVES USED IN THE PSYCHOPHYSICAL EXPERIMENT

Rough	Smooth
Bumpy	Flat
Sticky	Slippery
Soft	Hard
Warm	Cold
Stiff	Elastic
Regular	Irregular
Fine	Coarse

E. Experimental procedure

Participants were asked to execute different exploratory patterns (pressure and lateral motion) with the pen in their dominant hand, while interacting with a graphical user interface. The experiment consisted of three sessions, and the following tasks had to be performed in each session.

Each participant sat in front of the experimental setup in a comfortable position. At the beginning of each trial, they pressed the start button and heard a sound cue which indicated the start of the trial. After this, they pressed three times on the screen with the pen on the left part of the cutout while trying to reach the 1.5 N pressing force level on a force gauge. They were also asked to hold the device perpendicular to the screen while pressing. After the third press, they stayed at the 1N level indicated by the force gauge. Then, after another sound cue, the ball on the GUI turned green and started moving back and forth with a constant speed of 50 mm/s. The task was to follow this green ball while sliding on the screen with the pen, trying to maintain a constant applied force at around 1N. The ball went back and forth twice from left to right. The end of the trial was indicated by another sound cue. After this, participants rated the textures on the 16 adjectives by moving sliders on the adjective scales. Once they were ready, they clicked on the ready checkbox and pressed the next trial button to proceed to the next trial. Each trial could be played at a maximum of two times and there were no time constraints on the duration of ratings.

The first session was a test session with 10 trials, giving the participants 10 noticeably distinct stimuli. This test session helped them become comfortable with the experimental setup and the procedure, as well as ensured that they were acquainted with a wide range of textures. They were asked to rate the textures in the next two sessions based on the stimuli in this test session. Their ratings in this session were not recorded.

The 60 stimuli were divided into two sets of 30 trials in two consecutive sessions, with a 5-10 minute break in between. The order of stimuli were randomized in both sessions. Participants rated each of the 60 artificial textures on each of the 16 sensory adjective scales. The scales were dimensionless with their two ends labeled as max and min. Participants gave their answers based on how strongly the given adjective described the given texture. The duration of each 30-trial session was about 30-45 minutes, and the entire experiment lasted around 1.5-2 hours. The 60 x 16 = 960 sensory adjective ratings from each participant were the primary data for analysis.

F. Data analysis

The adjective ratings were standardized by calculating z-scores of each adjective scale within participants. The standardized adjective ratings were then averaged across all subjects, resulting in a 60×16 matrix (number of stimuli × number of adjectives).

This matrix was analysed by a principal component analysis (PCA). We analysed whether the data was applicable for PCA using the Keyser-Meyer-Olkin (KMO) criterion and Bartlett's test of sphericity. Bartlett's test of sphericity tests the null hypothesis that the correlation matrix is an identity matrix. A significant test shows that the correlation matrix is indeed not an identity matrix, so the variables can be purposely analysed by PCA. The KMO criterion measures sampling adequacy that indicates the proportion of variance in the variables that might be caused by underlying factors. KMO score takes values between 0 and 1, and the higher the KMO score, the more suited the data to PCA. Principal components were extracted by using the Kaiser-criterion and the scree plot, and rotated using the varimax method [11].

Finally, Pearson correlation coefficients between the parameters of the texture design space and the standardized adjective ratings were calculated to see how each parameter affects the ratings of different adjectives.

VI. Results

A. Principal component analysis on sensory adjectives

To study the feasibility of the device for rendering major psychophysical dimensions, a principal component analysis was conducted on the average adjective scores. The KMO score had a value of 0.759, indicating a "middling" suitability for PCA. Bartlett's test of sphericity was significant, $\chi^2 = 1739.47$, $p < 0.001$, so there are meaningful correlations across adjectives. We extracted four principal components according to the Kaiser-criterion and looking at the scree plot, which explained 93.64% of the total variance.

We applied varimax rotation on the component matrix. The goal of rotation is to improve the interpretability of the component matrix by reaching simple structure (see Table IV for the rotated component matrix with the four components and the component loadings). The biplot in Figure 7 projects the individual observations and the component loadings for the first two components. Each component is described through the adjectives using the following criteria: (1) the absolute value of the component loading is >0.75 for the adjective and (2) the loading is higher on that component than on any other component.

The first rotated component explains 31.6% of the total variance. It is described by adjectives "bumpy", "flat", "regular", "irregular", "fine" and "coarse". These adjectives seem to carry macroscopic texture properties similar to gratings in real materials, so this component could be interpreted as the virtual equivalent of macroscopic roughness. The second rotated component explains 25.3% of the total variance and it is described by "rough", "smooth", "sticky" and "slippery" adjectives. There is also a moderate loading on "fine" and "coarse" adjectives. This component seems to associate to the combination of microscopic roughness and friction dimensions. The third rotated component explains 24.3% of the total variance and is defined by "soft", "hard", "stiff" and "elastic" adjectives. This component seems to link to the softness/hardness material property. The fourth rotated component explains 12.5% of the total variance and is described by "warm" and "cold" adjectives. Altogether, this component relates to the perceptual dimension of coldness/warmth.

TABLE IV
ROTATED COMPONENT MATRIX

Adjectives	Components			
	1	2	3	4
Rough	-0.242	0.928	0.080	0.012
Smooth	0.296	-0.929	-0.039	0.022
Bumpy	-0.935	0.024	0.012	0.121
Flat	0.930	-0.057	-0.029	-0.144
Sticky	-0.007	0.904	0.267	-0.031
Slippery	0.035	-0.942	-0.233	0.016
Soft	0.022	-0.187	-0.960	-0.038
Hard	-0.033	0.157	0.972	0.028
Warm	-0.128	-0.035	0.013	0.982
Cold	0.110	-0.005	0.012	-0.985
Stiff	-0.010	0.141	0.970	0.007
Elastic	0.083	-0.099	-0.951	0.065
Regular	0.959	-0.062	0.024	0.002
Irregular	-0.957	0.097	0.005	-0.006
Fine	0.825	-0.459	-0.137	-0.097
Coarse	-0.787	0.543	0.144	0.111

B. Correlations between texture parameters and adjective ratings

Figure 8 shows the correlation coefficients between the texture parameters and the sensory adjective ratings. The amplitude of the voltage signal moderately correlated with roughness and stickiness, and there was a moderate negative correlation with smoothness and slipperiness. This result seems plausible, as the signal amplitude modifies the magnitude of adhesion between the stylus tip and the touchscreen.

Continuing with the frequency of the voltage signal, there was a moderate correlation with smoothness and moderate

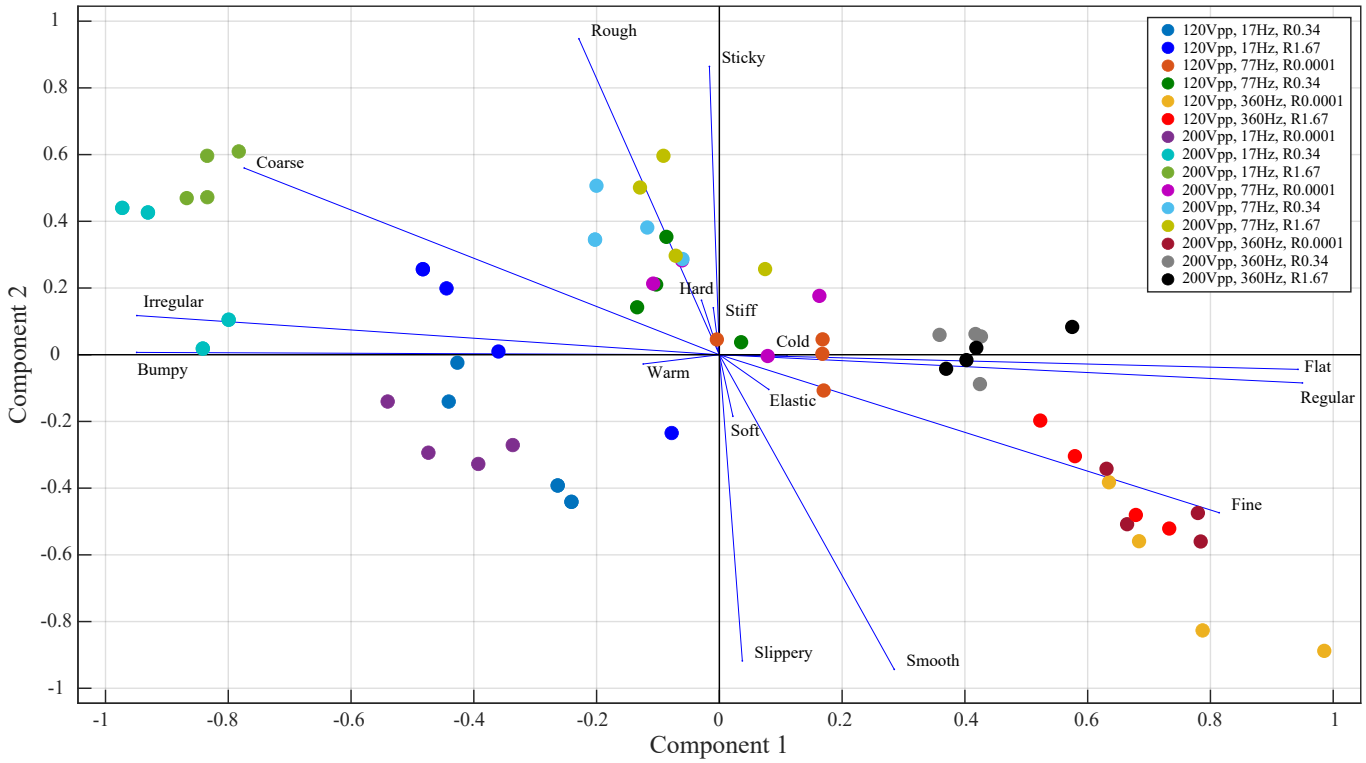

Fig. 7. Biplot visualizing component loadings and component scores of the first two components. The observations related to the electrovibration display are colour coded.

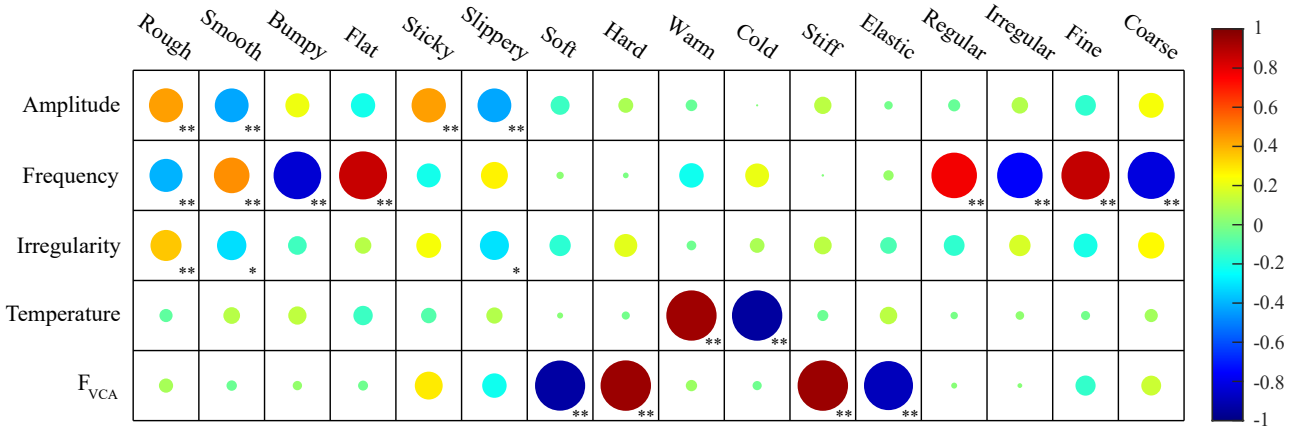

Fig. 8. Correlation matrix, showing the correlation between sensory adjectives and texture parameters. ** $p < 0.01$ and * $p < 0.05$.

negative correlation with roughness. The signal frequency highly correlated with flatness, regularity and fineness, and there was a negative high correlation with bumpiness, irregularity and coarseness. These adjectives are all related to some extent to the granular properties of texture surfaces. Of course, this granular property can only be associated with virtual gratings on an electrovibration display.

There is only a moderate correlation/negative correlation between irregularity and rough/smooth adjectives. Interestingly, there is only a low correlation with regular/irregular adjectives. The high correlation between frequency and the regular/irregular adjectives indicates that the irregularity parameter alone does not sufficiently alter our perception of texture regularity.

There was a high degree of negative correlation between the temperature of the thermal module and coldness sensation, and a high degree of negative correlation with warmness sensation. This high correlation demonstrates the good performance of the thermal module.

The exerted force of the voice coil actuator correlates highly with hardness and stiffness, and there is a high negative correlation with softness and elasticity. This shows that acting against the various stroke force levels of the voice-coil actuator captures softness perception fairly well.

VII. Discussion

This study presents a novel haptic interface capable of conveying multimodal texture properties. We characterized the device from three aspects: (1) performance of the thermal module, (2) force characteristics of the voice-coil actuator and (3) magnitudes of electrovibration force and friction coefficients of the pen-electrostatic display interaction. Our results from the psychophysical experiment revealed four perceptual dimensions, with the first two related to texture surface properties, and the third and fourth dimensions linked to material softness and coldness, respectively.

A. Characterization experiments

The measurements conducted on the thermal module showed a good overall performance in the 15-40 °C range, which was chosen to avoid the sensation of pain [27]. Negative steps produced a faster tracking performance, in contrast to the findings in [47]. This can be due to the fact that we took the measurements while the finger was in constant contact with the module.

The mean absolute errors in Table I indicate the validity of the dynamic model of the voice coil actuator. There is a slight difference between the measured and simulated maximum force values. This can be explained by the fact that the thermal part was not implemented in the model, which would cause a slight decrease in the maximum force over time.

The characterization experiment of the pen-electrostatic display interaction revealed some apparent trends, although further analysis would be needed for factual findings. The EV force amplitude increases as a function of input voltage signal amplitude. As the alternating electrovibration force induces the perception [48] and there are significant correlations between intensity perception and voltage amplitude, our results seem plausible. The EV force amplitude also increases as a function of applied normal force on the screen, which is in good agreement with previous studies [51], [52]. Scanning speed seems to have little effect on EV force amplitude, except for some lower frequencies. The friction coefficients increase with the normal force at 50 mm/s scanning speed, although an opposite trend can be observed for 100 mm/s scanning speed. Interestingly, the friction coefficients are lower compared to the no voltage case at 100 mm/s scanning speed. These unexpected findings indicate that further investigation is needed to understand the pen tip - display interaction, which seems to be somewhat different from the interaction with finger.

B. Psychophysical experiment

By looking at the rotated component matrix in Table IV and the correlation matrix in Figure 8, we can connect which parameters have the greatest effect on each dimension. Frequency seems to be a salient texture parameter, as it has a high correlation with the adjectives (flat, regular, fine) describing the first perceptual dimension. This finding is in good agreement with previous studies that also found frequency to be one of the key parameters in synthetic texture saliency [36], [38]. Our results also show that the perceived sensations feel less bumpy, coarse and irregular with increasing voltage signal frequency.

The second dimension is best described by the rough-smooth and sticky-slippery adjective pairs. The sticky and slippery adjectives correlate best with the amplitude of the voltage signal. This seems plausible, as a higher voltage amplitude implies greater electrostatic adhesion between the stylus tip and the touchscreen. Interestingly, roughness ratings correlate with all three surface texture parameters, amplitude, frequency and irregularity, although these correlations are only moderate. In general, higher irregularity values implied an increase in roughness sensation. This can be explained by the increased signal power due to the added frequency components, which is known to be an appropriate metric for roughness perception [24].

The current set of parameters revealed only two dimensions on the electrovibration display. The texture set of Mun et al. using tessellations of polygons was found to be three-dimensional, namely rough-smooth, dense-sparse and bumpy-even [35]. The discrepancy can be caused by the difference between the experimental methods: they used five parameters to alter their stimuli, the dimensions were obtained by multidimensional scaling method and different adjectives were used to rate the textures. These differences highlight that, in our case, additional dimensions might be acquired by using an even broader set of voltage signal parameters.

Moving on to the third dimension, it is best explained by softness perception. The high correlations between the stroke force of the VCA and the adjectives describing softness material properties indicate that our design effectively exploits the kinesthetic softness perception. Although LaMotte found that the discrimination of softness is better for tapping than for pressing with a stylus, the softness of objects can still be discriminated when there is already a contact while actively pressing on them [32], [33]. We alter softness perception based on the ratio of the indentation depth of the stylus and the exerted force on the skin, providing higher force levels to act against for harder materials.

The fourth dimension can be best described by coldness sensation. Yamamoto et al. believe that the early times sensation phase plays an important role in material recognition, as there is a rapid temperature change in that phase which invokes a stronger sensation [28]. We exploited this phenomenon by applying step reference signals to the thermal module, providing fast initial temperature changes on the fingertip.

C. Limitations, suggestions and future extensions

Although we demonstrated that FeelPen is capable of conveying four perceptual dimensions, both the study and the design have their own limitations. The number of texture parameters were reduced due to time constraints of the psychophysical experiment, and a wider range of stimuli could reveal even more dimensions, as we saw in [35]. Moreover, the semantic differential method is prone to avoid certain dimensions if the adjectives are not chosen wisely [8].

To further facilitate the thermal perception with the device, a larger Peltier cell could be applied on top of the heat sink, taking advantage of the spatial summation effect [29]. As for the softness rendering, the maximum exerted force (2.3N) of

the VCA limits the maximum controllable stiffness of the device. Harder materials can be rendered by reversing the current direction inside the VCA, in this case the moving part hits a limiter and cannot be indented. Furthermore, to model materials with desired stiffness values, the indentation of the pen also needs to be measured with an IR sensor. Also, current drive would yield a simpler control algorithm for commanding the desired force values, as the generated force of the VCA is directly related to the current. The results from the characterization of pen-display interaction raise the need to develop a model similar to [48], [53] and make electrical impedance measurements to explain possible changes in the electrical circuit during the interaction. We hypothesize that the pen tip material has a crucial effect on perception.

In this study, we only rendered parametric artificial textures. However, the possibility is there to gather data from real-world materials and render these textures on the electrovibration display. It would be interesting to see whether texture realism increases with the new dimensions of FeelPen.

VIII. Conclusion

This paper presented a novel pen-type multimodal haptic interface with the aim to display augmented texture feels on touchscreens. We characterized the device to determine its physical characteristics and limitations. Moreover, we ran a psychophysical experiment to find the perceptual dimensions of FeelPen by making subjects rate artificial textures on a set of adjective scales. Based on our results, we can conclude the following.

- To the best of our knowledge, this is the first multimodal stylus that is able to convey sensations for four perceptual dimensions on a touchscreen.
- The first two dimensions are related to texture surface properties (explaining 56.9% of the total variance combined), and the third and fourth dimensions are linked to material softness and coldness, respectively. Although coldness seems to augment the texture feels, this dimension only explains 12.5% of the total variance.
- The correlations between sensory adjectives and the five texture design parameters give insight on which parameters to change to achieve a certain sensation.

Potential applications of the FeelPen may include immersive gaming experience on mobile devices, augmented texture feels during online shopping or painting in a graphic design software, as well as various AR and VR applications for entertainment and educational purposes.

Acknowledgment

The authors would like to thank Andres Hunt and Rebecca Fenton Friesen for their insights and fruitful discussions on the device design and rendering processes, respectively.

References

[1] A. Arasan, C. Basdogan, and T. M. Sezgin, "Haptistylus: A novel stylus for conveying movement and rotational torque effects," *IEEE Computer Graphics and Applications*, vol. 36, no. 1, pp. 30–41, 2015.

[2] Z. F. Quek, S. B. Schorr, I. Nisky, A. M. Okamura, and W. R. Provancher, "Augmentation of stiffness perception with a 1-degree-of-freedom skin stretch device," *IEEE Transactions on Human-Machine Systems*, vol. 44, no. 6, pp. 731–742, 2014.

[3] D. Wang, K. Ohnishi, and W. Xu, "Multimodal haptic display for virtual reality: A survey," *IEEE Transactions on Industrial Electronics*, vol. 67, no. 1, pp. 610–623, 2019.

[4] H. Culbertson and K. J. Kuchenbecker, "Ungrounded haptic augmented reality system for displaying roughness and friction," *IEEE/ASME Transactions on Mechatronics*, vol. 22, no. 4, pp. 1839–1849, 2017.

[5] H. Culbertson and K. J. Kuchenbecker, "Importance of matching physical friction, hardness, and texture in creating realistic haptic virtual surfaces," *IEEE Transactions on Haptics*, vol. 10, no. 1, pp. 63–74, 2016.

[6] D. Chen, A. Song, L. Tian, Y. Yu, and L. Zhu, "Mh-pen: A pen-type multi-mode haptic interface for touch screens interaction," *IEEE Transactions on Haptics*, vol. 11, no. 4, pp. 555–567, 2018.

[7] T. Nakamura and A. Yamamoto, "Extension of an electrostatic visuo-haptic display to provide softness sensation," in *2016 IEEE Haptics Symposium (HAPTICS)*. IEEE, 2016, pp. 78–83.

[8] S. Okamoto, H. Nagano, and Y. Yamada, "Psychophysical dimensions of tactile perception of textures," *IEEE Transactions on Haptics*, vol. 6, no. 1, pp. 81–93, 2012.

[9] S. J. Lederman and R. L. Klatzky, "Hand movements: A window into haptic object recognition," *Cognitive psychology*, vol. 19, no. 3, pp. 342–368, 1987.

[10] T. Yoshioka, S. J. Bensmaia, J. C. Craig, and S. S. Hsiao, "Texture perception through direct and indirect touch: An analysis of perceptual space for tactile textures in two modes of exploration," *Somatosensory & motor research*, vol. 24, no. 1-2, pp. 53–70, 2007.

[11] K. Drewing, C. Weyel, H. Celebi, and D. Kaya, "Systematic relations between affective and sensory material dimensions in touch," *IEEE Transactions on Haptics*, vol. 11, no. 4, pp. 611–622, 2018.

[12] A. R. Rao and G. L. Lohse, "Towards a texture naming system: Identifying relevant dimensions of texture," *Vision Research*, vol. 36, no. 11, pp. 1649–1669, 1996.

[13] M. Hollins, R. Faldowski, S. Rao, and F. Young, "Perceptual dimensions of tactile surface texture: A multidimensional scaling analysis," *Perception & psychophysics*, vol. 54, no. 6, pp. 697–705, 1993.

[14] D. Katz and L. E. Krueger, *The world of touch*. Psychology press, 2013.

[15] S. J. B. Hollins and M. Sean Washburn, "Vibrotactile adaptation impairs discrimination of fine, but not coarse, textures," *Somatosensory & motor research*, vol. 18, no. 4, pp. 253–262, 2001.

[16] S. J. Lederman, "Tactile roughness of grooved surfaces: The touching process and effects of macro-and microsurface structure," *Perception & Psychophysics*, vol. 16, no. 2, pp. 385–395, 1974.

[17] S. J. Lederman, "Tactual roughness perception: spatial and temporal determinants." *Canadian Journal of Psychology/Revue canadienne de psychologie*, vol. 37, no. 4, p. 498, 1983.

[18] C. J. Cascio and K. Sathian, "Temporal cues contribute to tactile perception of roughness," *Journal of Neuroscience*, vol. 21, no. 14, pp. 5289–5296, 2001.

[19] A. M. Smith, C. E. Chapman, M. Deslandes, J.-S. Langlais, and M.-P. Thibodeau, "Role of friction and tangential force variation in the subjective scaling of tactile roughness," *Experimental brain research*, vol. 144, no. 2, pp. 211–223, 2002.

[20] M. Hollins and S. R. Risner, "Evidence for the duplex theory of tactile texture perception," *Perception & psychophysics*, vol. 62, no. 4, pp. 695–705, 2000.

[21] R. L. Klatzky, S. J. Lederman, C. Hamilton, M. Grindley, and R. H. Swendsen, "Feeling textures through a probe: Effects of probe and surface geometry and exploratory factors," *Perception & psychophysics*, vol. 65, no. 4, pp. 613–631, 2003.

[22] B. Unger, R. Hollis, and R. Klatzky, "Roughness perception in virtual textures," *IEEE Transactions on Haptics*, vol. 4, no. 2, pp. 122–133, 2010.

[23] A. İşleyen, Y. Vardar, and C. Basdogan, "Tactile roughness perception of virtual gratings by electrovibration," *IEEE Transactions on Haptics*, vol. 13, no. 3, pp. 562–570, 2019.

[24] Y. Vardar, A. İşleyen, M. K. Saleem, and C. Basdogan, "Roughness perception of virtual textures displayed by electrovibration on touch screens," in *2017 IEEE World Haptics Conference (WHC)*. IEEE, 2017, pp. 263–268.

[25] X. Liu, Z. Yue, Z. Cai, D. Chetwynd, and S. Smith, "Quantifying touch–feel perception: tribological aspects," *Measurement Science and Technology*, vol. 19, no. 8, p. 084007, 2008.

[26] J. van Kuilenburg, M. A. Masen, and E. van der Heide, "A review of fingerpad contact mechanics and friction and how this affects tactile perception," *Proceedings of the Institution of Mechanical Engineers, Part J: Journal of engineering tribology*, vol. 229, no. 3, pp. 243–258, 2015.

[27] I. Darian-Smith and K. O. Johnson, "Thermal sensibility and thermoreceptors," *Journal of Investigative Dermatology*, vol. 69, no. 1, pp. 146–153, 1977.

[28] A. Yamamoto, B. Cros, H. Hashimoto, and T. Higuchi, "Control of thermal tactile display based on prediction of contact temperature," in *IEEE International Conference on Robotics and Automation, 2004. Proceedings. ICRA'04. 2004*, vol. 2. IEEE, 2004, pp. 1536–1541.

[29] H.-N. Ho and L. A. Jones, "Contribution of thermal cues to material discrimination and localization," *Perception & Psychophysics*, vol. 68, no. 1, pp. 118–128, 2006.

[30] W. M. B. Tiest and A. M. Kappers, "Cues for haptic perception of compliance," *IEEE transactions on haptics*, vol. 2, no. 4, pp. 189–199, 2009.

[31] M. A. Srinivasan and R. H. LaMotte, "Tactual discrimination of softness," *Journal of neurophysiology*, vol. 73, no. 1, pp. 88–101, 1995.

[32] R. M. Friedman, K. D. Hester, B. G. Green, and R. H. LaMotte, "Magnitude estimation of softness," *Experimental brain research*, vol. 191, no. 2, pp. 133–142, 2008.

[33] R. H. LaMotte, "Softness discrimination with a tool," *Journal of neurophysiology*, vol. 83, no. 4, pp. 1777–1786, 2000.

[34] M. Dariosecq, P. Plénacoste, F. Berthaut, A. Kaci, and F. Giraud, "Investigating the semantic perceptual space of synthetic textures on an ultrasonic based haptic tablet," in *HUCAPP 2020*, 2020.

[35] S. Mun, H. Lee, and S. Choi, "Perceptual space of regular homogeneous haptic textures rendered using electrovibration," in *2019 IEEE World Haptics Conference (WHC)*. IEEE, 2019, pp. 7–12.

[36] I. Hwang, J. Seo, and S. Choi, "Perceptual space of superimposed dual-frequency vibrations in the hands," *PloS one*, vol. 12, no. 1, p. e0169570, 2017.

[37] R. F. Friesen, R. L. Klatzky, M. A. Peshkin, and J. E. Colgate, "Building a navigable fine texture design space," *IEEE Transactions on Haptics*, vol. 14, no. 4, pp. 897–906, 2021.

[38] C. Bernard, J. Monnoyer, and M. Wiertlewski, "Harmonious textures: The perceptual dimensions of synthetic sinusoidal gratings," in *International Conference on Human Haptic Sensing and Touch Enabled Computer Applications*. Springer, 2018, pp. 685–695.

[39] G. Ilkhani, M. Aziziaghdam, and E. Samur, "Data-driven texture rendering on an electrostatic tactile display," *International Journal of Human–Computer Interaction*, vol. 33, no. 9, pp. 756–770, 2017.

[40] R. H. Osgouei, J. R. Kim, and S. Choi, "Data-driven texture modeling and rendering on electrovibration display," *IEEE Transactions on Haptics*, vol. 13, no. 2, pp. 298–311, 2019.

[41] D. J. Meyer, M. Wiertlewski, M. A. Peshkin, and J. E. Colgate, "Dynamics of ultrasonic and electrostatic friction modulation for rendering texture on haptic surfaces," in *2014 IEEE Haptics Symposium (HAPTICS)*. IEEE, 2014, pp. 63–67.

[42] Q. Wang, X. Ren, S. Sarcar, and X. Sun, "Ev-pen: Leveraging electrovibration haptic feedback in pen interaction," in *Proceedings of the 2016 ACM international conference on interactive surfaces and spaces*, 2016, pp. 57–66.

[43] H. Kim, J. Kang, K.-D. Kim, K.-M. Lim, and J. Ryu, "Method for providing electrovibration with uniform intensity," *Ieee transactions on haptics*, vol. 8, no. 4, pp. 492–496, 2015.

[44] Y. Vardar, B. Güçlü, and C. Basdogan, "Effect of waveform on tactile perception by electrovibration displayed on touch screens," *IEEE transactions on haptics*, vol. 10, no. 4, pp. 488–499, 2017.

[45] A. Withana, M. Kondo, Y. Makino, G. Kakehi, M. Sugimoto, and M. Inami, "Impact: Immersive haptic stylus to enable direct touch and manipulation for surface computing," *Computers in Entertainment (CIE)*, vol. 8, no. 2, pp. 1–16, 2010.

[46] S. Nagasaka, Y. Uranishi, S. Yoshimoto, M. Imura, and O. Oshiro, "Haptic interface with a stylus for a mobile touch panel," *ITE Transactions on Media Technology and Applications*, vol. 3, no. 4, pp. 279–286, 2015.

[47] M. Gabardi, D. Leonardis, M. Solazzi, and A. Frisoli, "Development of a miniaturized thermal module designed for integration in a wearable haptic device," in *2018 IEEE Haptics Symposium (HAPTICS)*. IEEE, 2018, pp. 100–105.

[48] Y. Vardar and K. J. Kuchenbecker, "Finger motion and contact by a second finger influence the tactile perception of electrovibration," *Journal of the Royal Society Interface*, vol. 18, no. 176, p. 20200783, 2021.

[49] S. Guest, J. M. Dessirier, A. Mehrabyan, F. McGlone, G. Essick, G. Gescheider, A. Fontana, R. Xiong, R. Ackerley, and K. Blot, "The development and validation of sensory and emotional scales of touch perception," *Attention, Perception, & Psychophysics*, vol. 73, no. 2, pp. 531–550, 2011.

[50] E. Baumgartner, C. B. Wiebel, and K. R. Gegenfurtner, "Visual and haptic representations of material properties," *Multisensory research*, vol. 26, no. 5, pp. 429–455, 2013.

[51] X. Guo, Y. Zhang, D. Wang, L. Lu, J. Jiao, and W. Xu, "Correlation between electrovibration perception magnitude and the normal force applied by finger," in *International Conference on Human Haptic Sensing and Touch Enabled Computer Applications*. Springer, 2018, pp. 91–101.

[52] X. Guo, Y. Zhang, D. Wang, L. Lu, J. Jiao, and W. Xu, "The effect of applied normal force on the electrovibration," *IEEE Transactions on Haptics*, vol. 12, no. 4, pp. 571–580, 2019.

[53] C. D. Shultz, M. A. Peshkin, and J. E. Colgate, "Surface haptics via electroadhesion: Expanding electrovibration with johnsen and rahbek," in *2015 IEEE World Haptics Conference (WHC)*. IEEE, 2015, pp. 57–62.

A

TECHNICAL DRAWINGS OF THE HEAT SINK

The technical drawings of the heat sink can be found on the following three pages. The heat sink consists of three parts for easier manufacturability: main body, front and back. The aluminum parts are attached together with cyanoacrylate glue. The silicone tubes that connect to the front of the heat sink are also attached with cyanoacrylate glue. The heat sink was tested for several days before installation to avoid any leakage during later use.

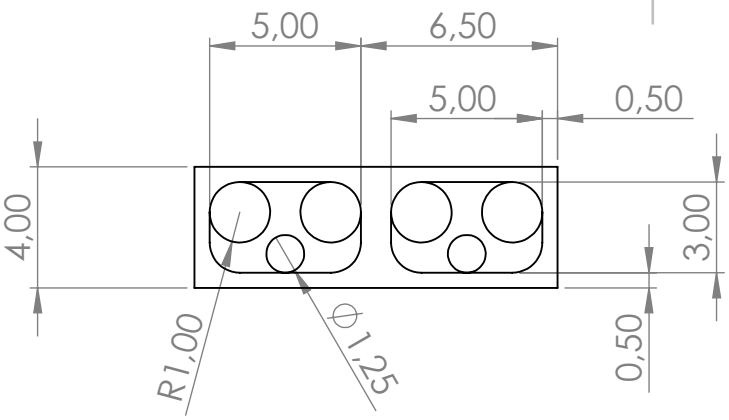

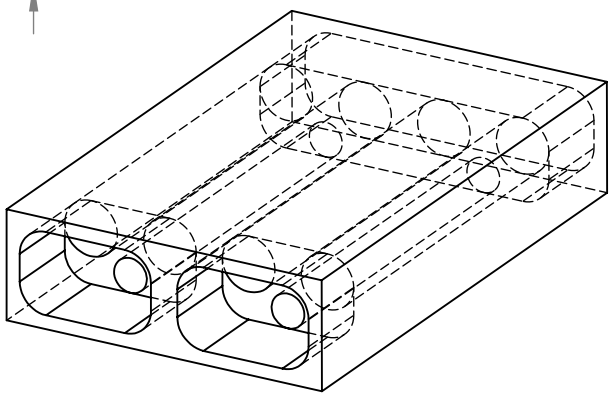

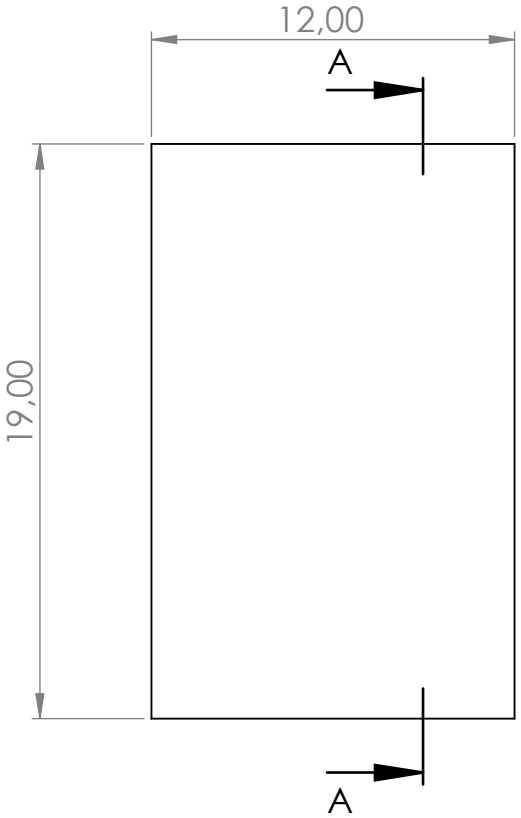

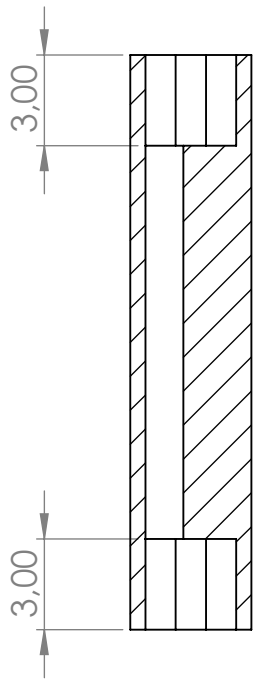

SECTION A-A

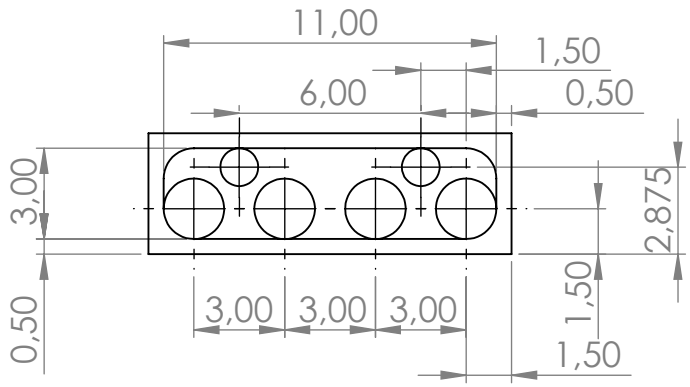

UNLESS OTHERWISE SPECIFIED: DIMENSIONS ARE IN MILLIMETERS SURFACE FINISH: TOLERANCES: LINEAR: ± 0.1 ANGULAR:	FINISH:	DEBURR AND BREAK SHARP EDGES	DO NOT SCALE DRAWING / REVISION

	NAME	SIGNATURE	DATE
DRAWN	Bence Kodak		21/07/21
CHK'D			
APPV'D			
MFG			
Q.A			

TITLE:

Heat sink

MATERIAL:

DWG NO.

heat_sink_FP

A4

WEIGHT:

SCALE:4:1

SHEET 1 OF 1

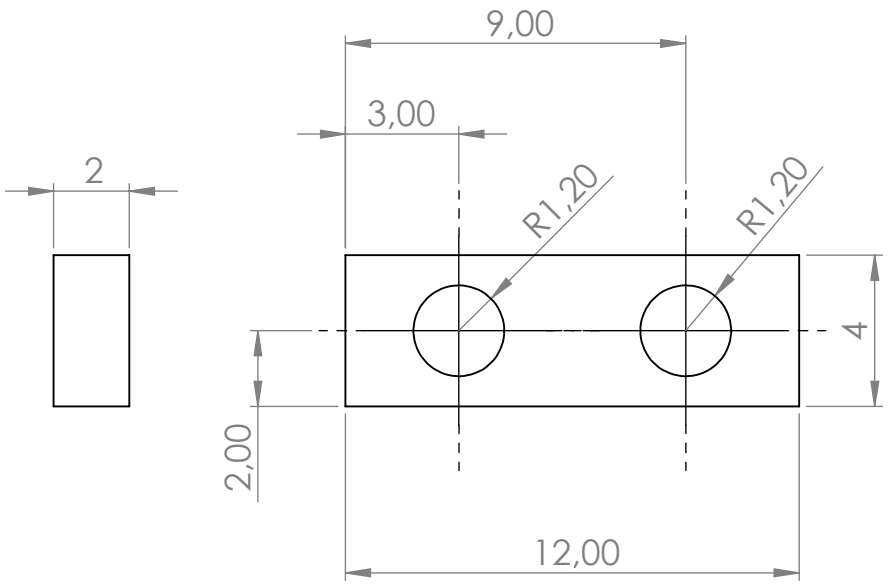

UNLESS OTHERWISE SPECIFIED: DIMENSIONS ARE IN MILLIMETERS SURFACE FINISH: TOLERANCES: LINEAR: ± 0.1 ANGULAR:		FINISH:		DEBURR AND BREAK SHARP EDGES		DO NOT SCALE DRAWING	REVISION
	NAME	SIGNATURE	DATE			TITLE:	
DRAWN	Bence Kodak		21/07/21			Heat sink front	
CHK'D							
APPV'D							
MFG							
Q.A				MATERIAL:		DWG NO.	A4
						heat_sink_front_FP	
				WEIGHT:		SCALE:5:1	SHEET 1 OF 1

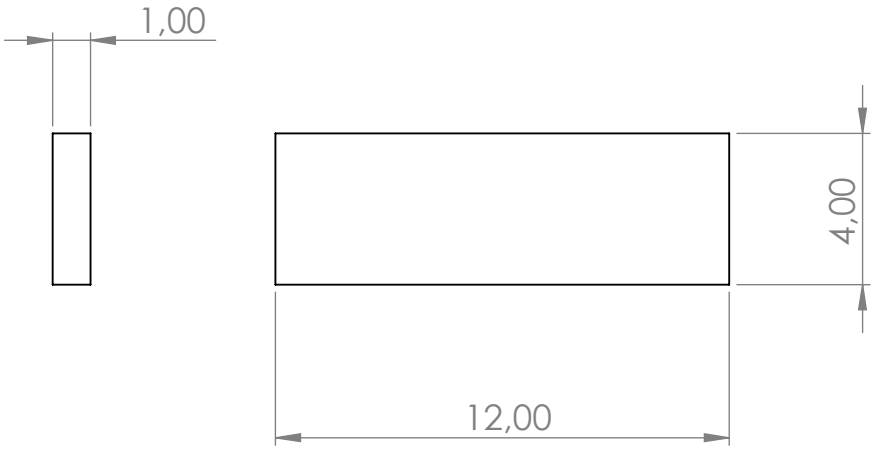

UNLESS OTHERWISE SPECIFIED: DIMENSIONS ARE IN MILLIMETERS SURFACE FINISH: TOLERANCES: LINEAR: ± 0.1 ANGULAR:		FINISH:		DEBURR AND BREAK SHARP EDGES		DO NOT SCALE DRAWING	REVISION
	NAME	SIGNATURE	DATE			TITLE:	
DRAWN	Bence Kodak		21/07/21			Heat sink back	
CHK'D							
APPV'D							
MFG							
Q.A				MATERIAL:		DWG NO.	A4
						heat_sink_back_FP	
				WEIGHT:		SCALE:5:1	SHEET 1 OF 1

B
PID PARAMETER SET

An asymmetric system behaviour between the cooling and warming phases led to the implementation of two sets of PID controller parameters and feed-forward gains. The coefficients of the Proportional (K_P), Integral (K_I) and Derivative (K_D) terms together with the Feed-Forward Gain (FF) can be seen in Table B.1.

Table B.1: Coefficients of the Proportional (K_P), Integral (K_I) and Derivative (K_D) terms together with the Feed-Forward Gain (FF), for both cooling and warming.

Side	K_P	K_I	K_D	FF
Cooling	1500	1	100	10
Warming	1800	4	200	-18

C

VOICE-COIL ACTUATOR PARAMETERS AND MEASUREMENTS

Table C.1: Parameters of the voice-coil actuator

Coil resistance [Ω]	11.3 ± 0.5
Coil inductance [mH]	1.93 ± 0.2
Force sensitivity, middle pos. [N/A]	$2.6 \pm 8\%$
BEMF constant, middle pos. [Vs/m]	$2.6 \pm 8\%$
Moving magnet mass [g]	$17.9 \pm 8\%$
Stroke length [mm]	18
$K_F(x)$ [N/A]	$-0.01x^2 - 0.00021x + 2.58$

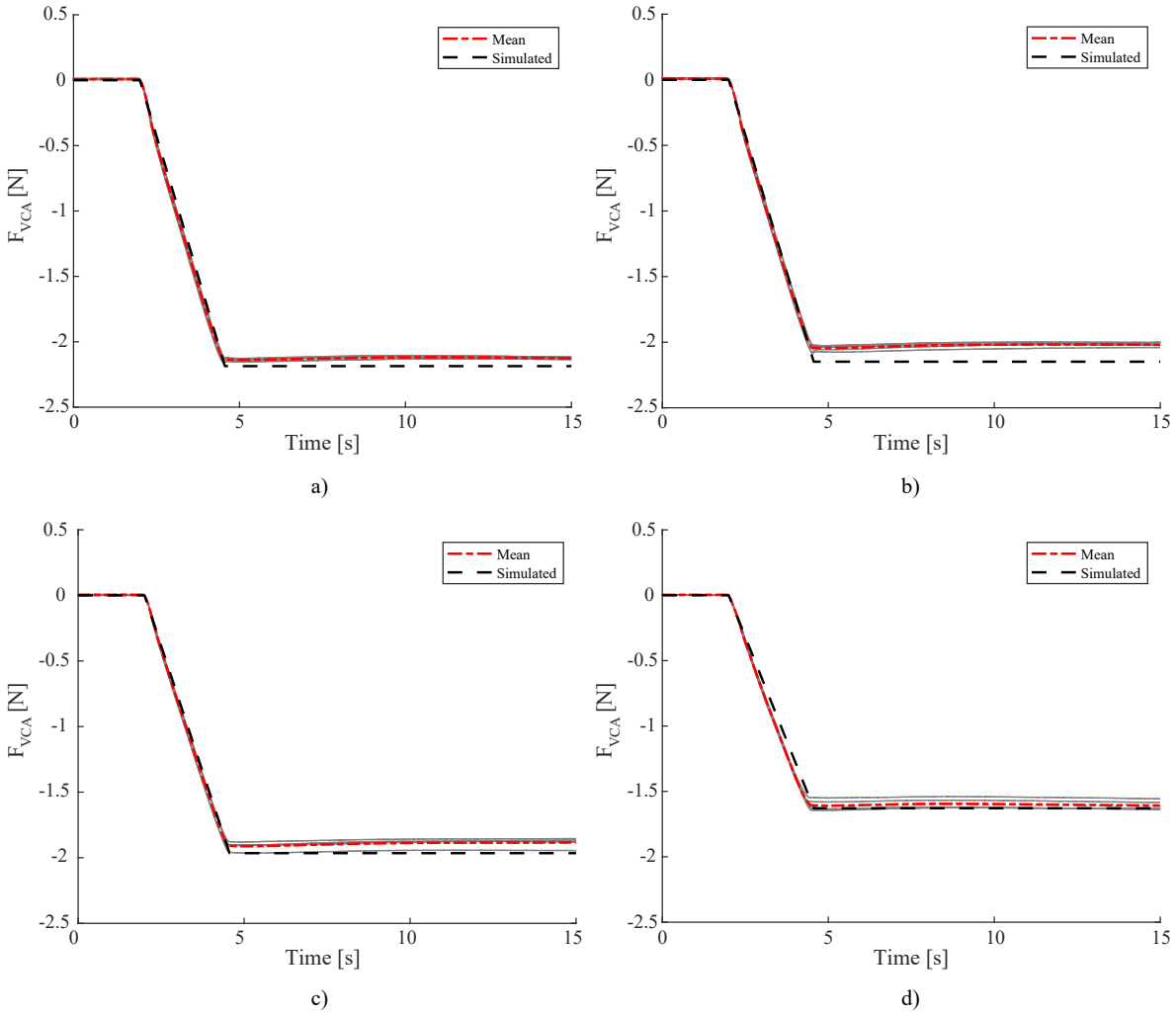

Figure C.1: Simulated and measured force characteristics of the voice-coil actuator for four initial positions: **a)** moving magnet is in the middle position, **b)** moving magnet is 2mm from the middle position, **c)** moving magnet is 5mm from the middle position and **d)** moving magnet is 8mm from the middle position. The grey lines represent the individual measurements.

D
ELECTROVIBRATION

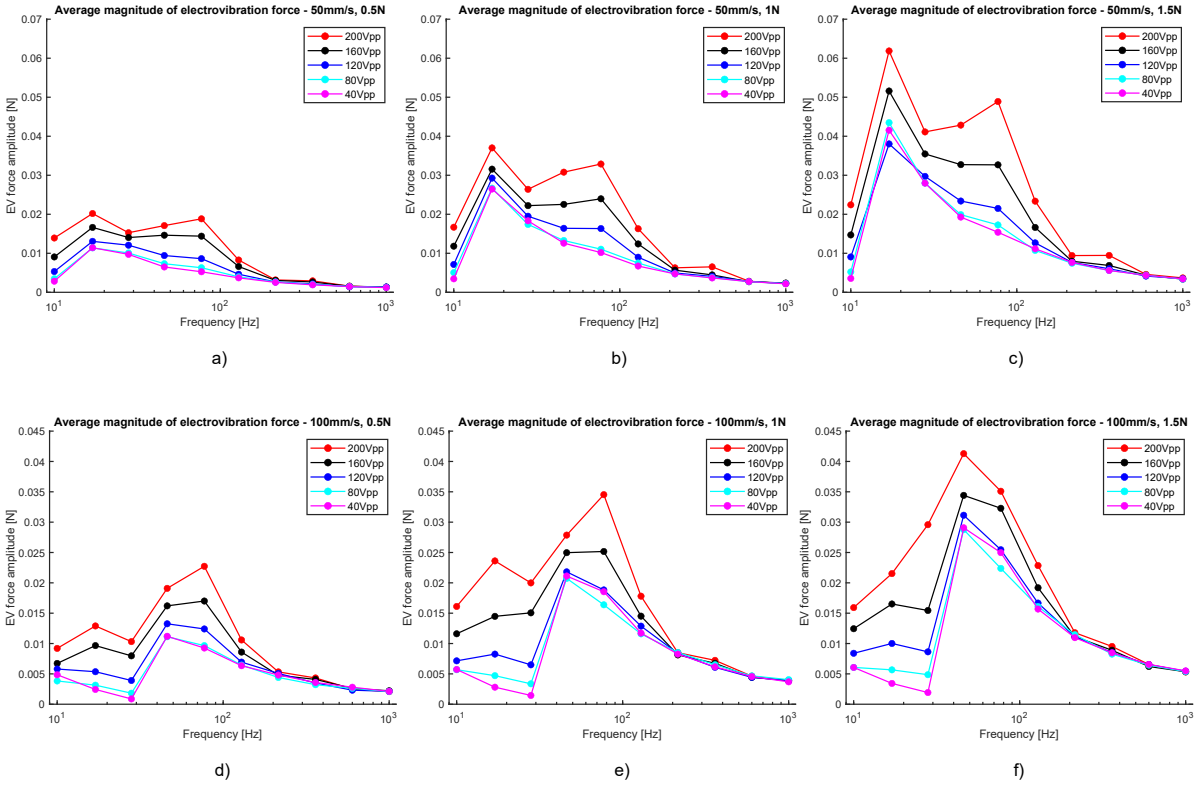

Figure D.1: Average magnitude of electrovibration force

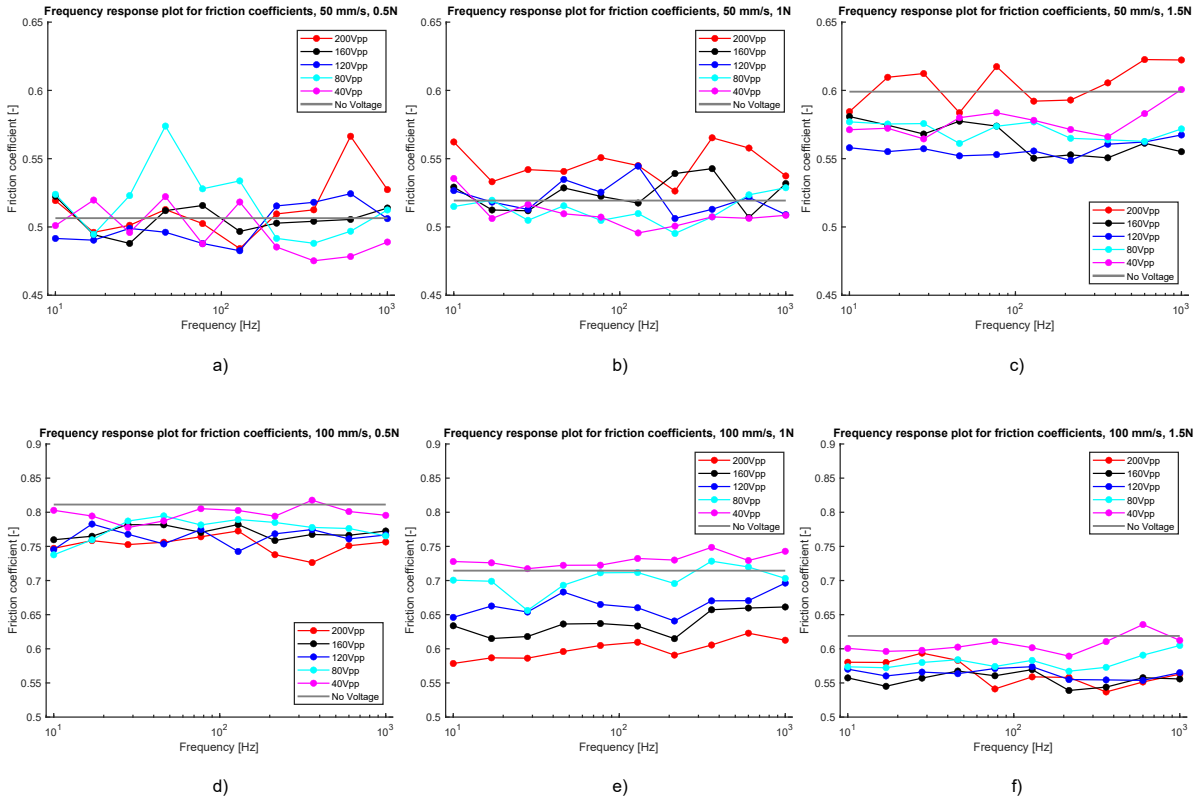

Figure D.2: Friction coefficients

E
STIMULI SET

Table E.1 shows the stimuli set used in the psychophysical experiment. The ten noticeably distinct stimuli used for the test sessions are highlighted in gray.

Table E.1: Parameter values of the stimuli set

Amplitude [Vpp]	Center frequency [Hz]	Irregularity [-]	Temperature level [°C]	Voltage on VCA [V]
120	17	0.34	24	10
120	17	0.34	28	3.1
120	17	0.34	40	3.1
120	17	0.34	40	10
120	17	1.67	24	10
120	17	1.67	28	3.1
120	17	1.67	28	10
120	17	1.67	40	3.1
120	77	0.0001	24	3.1
120	77	0.0001	28	10
120	77	0.0001	40	3.1
120	77	0.0001	40	10
120	77	0.34	24	3.1
120	77	0.34	28	3.1
120	77	0.34	28	10
120	77	0.34	40	10
120	360	0.0001	24	3.1
120	360	0.0001	24	10
120	360	0.0001	28	10
120	360	0.0001	40	3.1
120	360	1.67	24	3.1
120	360	1.67	24	10
120	360	1.67	28	3.1
120	360	1.67	40	10
200	17	0.0001	24	10
200	17	0.0001	28	3.1
200	17	0.0001	40	3.1
200	17	0.0001	40	10
200	17	0.34	24	10
200	17	0.34	28	3.1
200	17	0.34	28	10
200	17	0.34	40	3.1
200	17	1.67	24	3.1
200	17	1.67	28	10
200	17	1.67	40	3.1
200	17	1.67	40	10
200	77	0.0001	24	3.1
200	77	0.0001	28	3.1
200	77	0.0001	28	10
200	77	0.0001	40	10
200	77	0.34	24	3.1
200	77	0.34	24	10
200	77	0.34	28	10
200	77	0.34	40	3.1
200	77	1.67	24	3.1
200	77	1.67	24	10
200	77	1.67	28	3.1
200	77	1.67	40	10
200	360	0.0001	24	10
200	360	0.0001	28	3.1
200	360	0.0001	40	3.1
200	360	0.0001	40	10
200	360	0.34	24	3.1
200	360	0.34	28	3.1
200	360	0.34	28	10
200	360	0.34	40	10
200	360	1.67	24	3.1
200	360	1.67	24	10
200	360	1.67	28	10
200	360	1.67	40	3.1